

Effects of near-zero Dirac eigenmodes on axial $U(1)$ symmetry at finite temperature

Akio Tomiya^{*1}, Guido Cossu², Hidenori Fukaya¹, Shoji Hashimoto^{2,3}, Junichi Noaki²

¹*Department of Physics, Graduate School of Science, Osaka University, Toyonaka, Osaka 560-0043, Japan*

²*High Energy Accelerator Research Organization (KEK), Ibaraki 305-0801, Japan*

³*School of High Energy Accelerator Science, The Graduate University for Advanced Studies (Sokendai), Tsukuba 305-0801, Japan*

E-mail: akio@het.phys.sci.osaka-u.ac.jp

We study the axial $U(1)_A$ symmetry of $N_f = 2$ QCD at finite temperature using the Dirac eigenvalue spectrum. The gauge configurations are generated employing the Möbius domain-wall fermion action on $16^3 \times 8$ and $32^3 \times 8$ lattices. The physical spatial size of these lattices is around 2 fm and 4 fm, respectively, and the simulated temperature is around 200 MeV, which is slightly above the critical temperature of the chiral phase transition. Although the Möbius domain-wall Dirac operator is expected to have a good chiral symmetry and our data actually show small values of the residual mass, we observe significant violation of the Ginsparg-Wilson relation for the low-lying eigenmodes of the Möbius domain-wall Dirac operator. Using the reweighting technique, we compute the overlap-Dirac operator spectrum on the same set of configurations and find a significant difference of the spectrum between the two Dirac operators for the low-lying eigenvalues. The overlap-Dirac spectrum shows a gap from zero, which is insensitive to the spacial volume.

*The 32nd International Symposium on Lattice Field Theory,
23-28 June, 2014
Columbia University New York, NY*

^{*}Speaker.

1. Introduction

Two-flavor QCD Lagrangian in the vanishing quark mass limit has $SU(2)_L \times SU(2)_R \times U(1)_V \times U(1)_A$ symmetries. Among them, $U(1)_A$ is special because it is violated by the quantization of the theory, *i.e.* the chiral anomaly. Yet, whether and how anomaly affect the particle spectra are difficult questions. At zero temperature, it appears as the heavy η' mass compared to pions, while at high temperature it is under active research in the last couple of years.

In this work, we investigate the spectral density $\rho(\lambda)$ of the Dirac operator eigenvalue λ . It is related to the $U(1)_A$ symmetry through the relation,

$$\chi_\pi - \chi_\delta = \lim_{m \rightarrow 0} \int_0^\infty d\lambda \rho(\lambda) \frac{4m^2}{(m^2 + \lambda^2)^2}, \quad (1.1)$$

where χ_π and χ_δ are the susceptibilities of the isotriplet pseudoscalar and scalar operators respectively. When $\chi_\pi - \chi_\delta = 0$, the $U(1)_A$ breaking is invisible in the correlators of these channels. It was argued that if there is a gap in the Dirac spectrum, *i.e.* $\rho(\lambda) = 0$ for $\lambda < \lambda_{\text{gap}}$ with a finite λ_{gap} , $\chi_\pi - \chi_\delta$ vanishes [1]. It was further shown that if the $SU(2)_L \times SU(2)_R$ symmetry is fully restored above the critical temperature, the Dirac spectrum starts with at least cubic powers of λ and $\chi_\pi - \chi_\delta$ vanishes under this slightly relaxed assumption [2].

The Dirac spectrum can be investigated by numerical simulations of lattice QCD. The JLQCD collaboration [3] and TWQCD collaboration [4] reported that $U(1)_A$ symmetry is restored above the critical temperature using the overlap and the optimal domain-wall fermions, respectively. On the other hand, LLNL/RBC collaboration [5, 6] and Ohno *et. al* [7] obtained results that suggest the opposite conclusion using the domain-wall or staggered fermions. The former two groups employ the fermion action having better chirality, while the latter two groups performed the simulations on larger volumes. It is also noted that in [3] the global topological charge was fixed to zero.

In this work, we investigate the systematic effects which may result in the difference among the previous works, especially between the overlap and domain-wall type fermions. There are three possible causes. The first is the finite volume effect. There is always a gap in $\rho(\lambda)$ in the finite volume even below T_c . It is therefore important to carefully check the volume scaling of the gap if it exists. The second is the accuracy of the chiral symmetry. As [2] suggested, the full $SU(2)_L \times SU(2)_R$ symmetry plays a key role to suppress the $U(1)_A$ breaking effect in the correlators. The third is the effect of fixing topology.

We perform QCD simulations at around $T = 200$ MeV ($>T_c$) employing the Möbius domain-wall fermion action, which allows us to simulate QCD on larger volumes than that of the overlap fermion. The topological charge can change in this formulation. We use the code platform IroIro++ [8]. By the Möbius implementation of the domain-wall Dirac operator, we expect that the $SU(2)_L \times SU(2)_R$ symmetry is kept to a good precision. We also study the effect of small violation of their symmetry by reweighting the Möbius domain-wall Dirac determinant to that of the overlap Dirac operator. This reweighting, if realizes, corresponds to the dynamical overlap fermion simulation without fixing topology.

As we will see below, we found a significant difference between the Möbius domain-wall and the (reweighted) overlap-Dirac operator spectra. By checking the chirality of each eigenmode, it turned out that the low-modes of the Möbius domain-wall Dirac operator violate the Ginsparg-Wilson relation, quite significantly even when their contribution to the residual mass is small. Such

violation of the Ginsparg-Wilson relation in the low mode region may have a significant impact in the study of $SU(2)_L \times SU(2)_R$ and $U(1)_A$ symmetry restoration/breaking.

2. Lattice setup

2.1 Simulation with dynamical Möbius domain-wall quarks

We employ the Möbius domain-wall fermion action [9, 10] for the quarks. Its determinant is equivalent (except for overall constants) to that of a four-dimensional effective Dirac operator

$$D_{\text{DW}}^{4D}(m) = \frac{1+ma}{2} + \frac{1-ma}{2} \gamma_5 \text{sgn}_{\text{rat}}(H_M), \quad \text{sgn}_{\text{rat}}(H_M) = \frac{1 - (T(H_M))^{L_s}}{1 + (T(H_M))^{L_s}}, \quad (2.1)$$

$$T(H_M) = \frac{1-H_M}{1+H_M}, \quad H_M = \gamma_5 \frac{2aD_W}{2+aD_W}, \quad (2.2)$$

where D_W is the Wilson Dirac operator with a negative cut-off scale mass $-1/a$. We introduce three steps of the stout smearing for the gauge links. The residual mass, calculated as

$$m_{\text{res}} = \frac{\langle \text{tr} G^\dagger \Delta_L G \rangle}{\langle \text{tr} G^\dagger G \rangle}, \quad \Delta_L = \frac{1}{2} \gamma_5 (\gamma_5 D_{\text{DW}}^{4D} + D_{\text{DW}}^{4D} \gamma_5 - 2a D_{\text{DW}}^{4D} \gamma_5 D_{\text{DW}}^{4D}), \quad (2.3)$$

with G the contact-term-subtracted quark propagator, is roughly 5-10 times smaller than that of the conventional domain-wall Dirac operator for a fixed L_s , the size of fifth direction.

For the gauge part, we employ the Symanzik gauge action with $\beta = 4.07$ and 4.10. From the measurement of the Wilson flow at zero temperature the lattice spacing is estimated to be 0.135 fm and 0.125 fm, respectively. For each value of β , we simulate on two volumes $L^3 \times L_t = 16^3 \times 8$ and $32^3 \times 8$, at quark masses $am_{\text{ud}} = 0.01$ (30 MeV or 32 MeV) and $am_{\text{ud}} = 0.001$ (3.0 or 3.2 MeV). L_s is chosen such that the residual mass is kept at around or smaller than 1 MeV. From the Polyakov loop and the chiral condensate, the simulated temperature, 180 MeV ($\beta = 4.07$) and 200 MeV ($\beta = 4.10$), is estimated to be slightly above T_c . For each ensemble, we sample 50-200 gauge configurations from 100-700 trajectories of the hybrid Monte Carlo updates.

2.2 The overlap/domain-wall reweighting

In order to understand the difference between the domain-wall type fermions and the overlap fermions, we perform the reweighting of the dynamical Möbius domain-wall ensembles to those with the overlap Dirac operator determinant.

Our choice of the overlap Dirac operator is obtained by choosing a better approximation for the sign function in (2.1), while keeping the same kernel operator H_M . On the generated configurations, we compute lowest eigenmodes $|\lambda_i\rangle$ of the kernel operator H_M , and exactly calculate the sign function for them. Namely, we use

$$D_{\text{ov}}(0) = \frac{1}{2} \sum_{\lambda_i < |\lambda_{\text{th}}|} (1 + \gamma_5 \text{sgn} \lambda_i) |\lambda_i\rangle \langle \lambda_i| + D_{\text{DW}}^{4D}(0) (1 - \sum_{\lambda_i < |\lambda_{\text{th}}|} |\lambda_i\rangle \langle \lambda_i|), \quad (2.4)$$

where λ_i is the i -th lowest eigenvalue of H_M below a threshold λ_{th} . With our choice $a\lambda_{\text{th}} = 0.35$ (for $L = 16$) and 0.24 (for $L = 32$) the residual mass is negligible, *i.e.* $< 4 \times 10^{-3}$ MeV.

We perform the overlap/Möbius domain-wall reweighting by computing

$$\langle \mathcal{O} \rangle_{\text{ov}} = \left\langle \mathcal{O} \frac{\det D_{\text{ov}}^2(m_{\text{ud}})}{\det D_{\text{DW}}^2(m_{\text{ud}})} \frac{\det D_{\text{DW}}^2(1/2a)}{\det D_{\text{ov}}^2(1/2a)} \right\rangle_{\text{DW}}, \quad (2.5)$$

where the ratio of the determinants are stochastically estimated using $\mathcal{O}(10)$ noise samples for each configuration [11]. Here, $\langle \cdots \rangle_{\text{DW}}$ denotes the ensemble average on the dynamical Möbius domain-wall ensembles. Note that we have added an additional determinant of fermions and ghosts with a cut-off scale mass $(1/2a)$, which are irrelevant for the low-energy physics but effective in reducing statistical fluctuation originating from the UV modes.

It turned out that this overlap/Möbius domain-wall reweighting is effective only on the smaller lattice ($16^3 \times 8$). On the larger volume $32^3 \times 8$, we instead use the low-mode reweighting, *i.e.* approximating the determinants by a product of lowest $\mathcal{O}(10)$ eigenvalues. This is not a very precise approximation of the determinant but, as discussed later, can still be used to study the possible gap in the Dirac eigenvalue spectrum.

3. Preliminary results

3.1 Dirac spectrum

First, by comparing the spectrum of low-lying eigenvalues of $\gamma_5 D_{\text{DW}}(m)$ and that of the reweighted $\gamma_5 D_{\text{ov}}(m)$ measured on the same configurations, we examine the effect of the violation of chiral symmetry. Using the ensembles on two different lattice volumes, we can check the volume scaling at the same time. Since the configurations are generated with the Möbius domain-wall quark action, the topology tunneling is active.

Fig. 1 and 2 show the eigenvalue spectrum $\rho(\lambda)$ calculated on the $T = 180$ MeV lattices. Here, the i -th eigenvalue of massless Dirac operator λ_i is obtained by,

$$\lambda_i a \equiv \frac{\sqrt{a^2(\lambda_i^m)^2 - a^2 m_{\text{ud}}^2}}{\sqrt{1 - a^2 m_{\text{ud}}^2}}, \quad (3.1)$$

where λ_i^m is the i -th eigenvalue of massive hermitian Dirac operator $\gamma_5 D_{\text{DW}}^{4D}(m)$ or $\gamma_5 D_{\text{ov}}(m)$. When the quark mass is heavy, $m_{\text{ud}} \sim 30$ MeV, our data show apparent difference between the Möbius domain-wall and overlap Dirac eigenvalues near $\lambda \sim 0$ (Fig. 1). The left panel shows the data for $\gamma_5 D_{\text{DW}}^{4D}(0)$, while the right panel is those of (reweighted) $\gamma_5 D_{\text{ov}}(0)$. The overlap Dirac spectrum (right panel) has a peak around $\lambda \sim 0$, while the Möbius Domain-wall does not. The peak in the overlap spectrum originates from chiral zero-modes, which are determined unambiguously thanks to the nearly exact chiral symmetry of the overlap Dirac operator. Above the peak region, *i.e.* $\lambda a \sim 0.02$, the spectral density for the overlap becomes lower than that of Möbius domain-wall.

On the other hand, for the smaller $m_{\text{ud}} (\sim 3$ MeV) we do not find the peak after the reweighting, and the near-zero modes around $\lambda a \sim 0.01$ are washed out as shown in Fig. 2, where we present the data for $L \sim 2$ fm (top) and $L \sim 4$ fm (bottom). For the reweighted overlap, a gap ~ 20 MeV is found on both volumes, while the Möbius domain-wall spectrum shows eigenmodes below $|a\lambda| \approx 0.01$. On the large volume, in particular, there is an eigenvalue in the lowest bin. The data at $T \sim 200$ MeV are qualitatively similar.

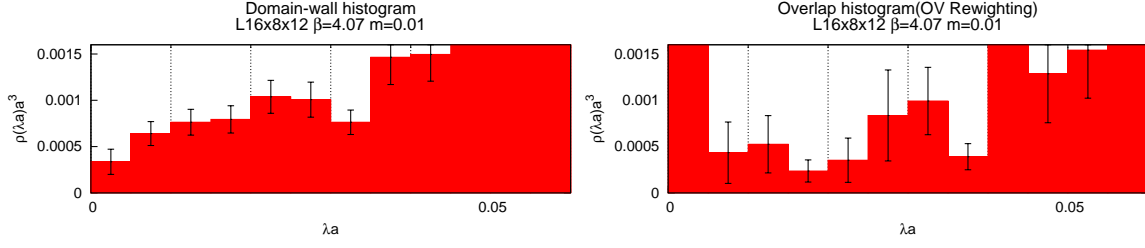


Figure 1: Eigenvalue spectrum of the Möbius domain wall (left panel) and reweighted overlap (right) Dirac operators. The data for $am_{\text{ud}} = 0.01$, $T \sim 180$ MeV on the $L^3 = 16^3 \times 8$ lattices. The peak in the lowest bin in the right panel is $a^3 p(0) = 0.00164 \pm 0.00045$.

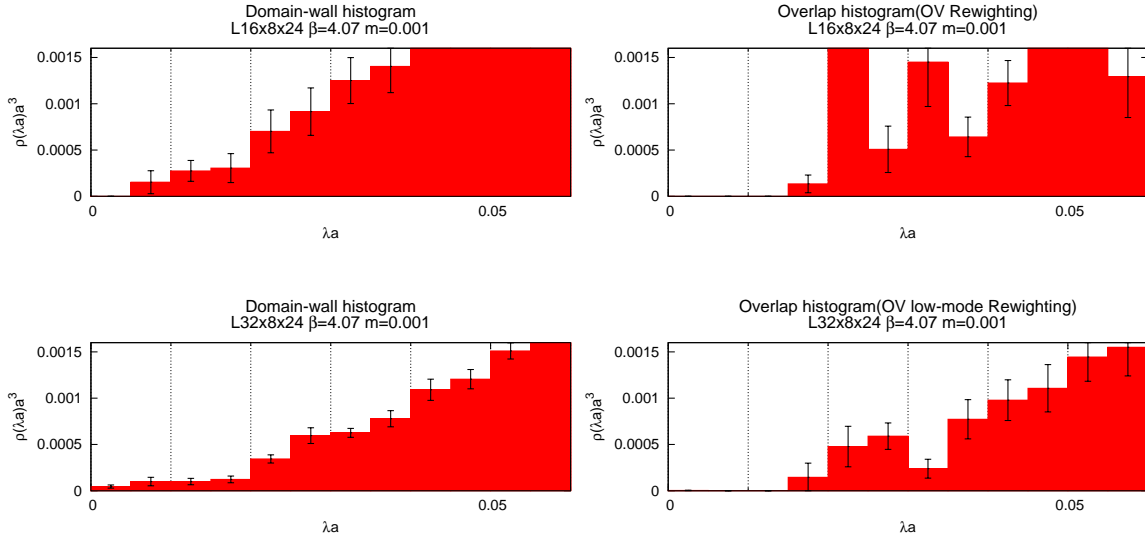


Figure 2: Eigenvalue spectrum of the Möbius domain wall (left panels) and reweighted overlap (right) Dirac operators. The data for $am_{\text{ud}} = 0.001$, $T \sim 180$ MeV on the $L^3 = 16^3 \times 8$ (top panels) and $L^3 = 32^3 \times 8$ (bottom) lattices are presented.

The reweighted overlap Dirac spectrum shows a gap, which is apparently insensitive to the volume. We may conclude that the difference from the Möbius domain-wall fermion is mainly due to the violation of the chiral symmetry, that we investigate in more detail below.

3.2 Violation of the Ginsparg-Wilson relation

We measure the violation of the Ginsparg-Wilson relation on each eigenmode of the Hermitian Dirac operator through

$$g_i \equiv \frac{\psi_i^\dagger \gamma_5 [D \gamma_5 + \gamma_5 D - 2aD \gamma_5 D] \psi_i}{\lambda_i^m} \left[\frac{(1 - am_{\text{ud}})^2}{2(1 + am_{\text{ud}})} \right], \quad (3.2)$$

where λ_i^m , ψ_i denotes the i -th eigenvalue/eigenvector of massive hermitian Dirac operator respectively. Last factor in (3.2) comes from the normalization of the Dirac operator. Note that one can

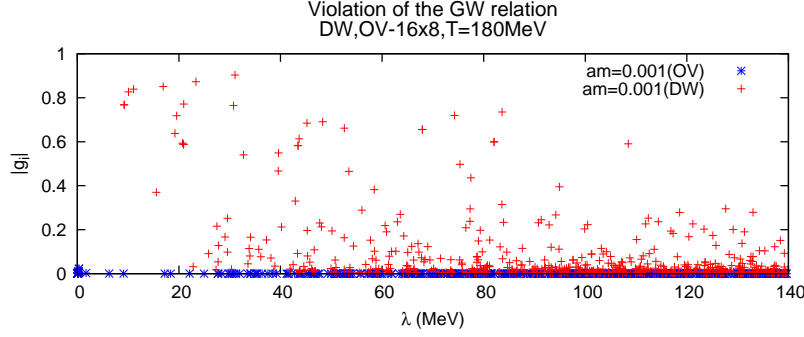


Figure 3: Violation of the Ginsparg-Wilson relation g_i for individual eigenmode. Pluses represent the Möbius domain-wall eigenvectors, while stars show the overlap eigenvectors, which are of course zero.

obtain the residual mass by an weighted average of g_i ,

$$m_{\text{res}} = \frac{\langle \text{tr} G^\dagger \Delta_L G \rangle}{\langle \text{tr} G^\dagger G \rangle} = \sum_i \frac{\lambda_i^m (1 + am_{\text{ud}})}{(1 - am_{\text{ud}})^2 (a\lambda_i^m)^2} g_i \bigg/ \sum_i \frac{1}{(a\lambda_i^m)^2}. \quad (3.3)$$

where the sum runs over all eigenvalues.

Figure 3 shows $|g_i|$ for each eigenvalue on the configuration of $16^3 \times 8$ and $m_{\text{ud}} \sim 3$ MeV. For the Möbius domain-wall fermion (crosses), the low-lying modes violate the chiral symmetry to the order of one, which means that the expectation value of $D\gamma_5 + \gamma_5 D - 2aD\gamma_5 D$ is of the same order of λ . The violation is of course negligible for the overlap fermion (stars). This result indicates that the low modes of the Möbius domain-wall Dirac operator contain substantial lattice artifact. Such lattice artifacts may also distort the eigenvalues, and explain the difference from the overlap operator.

3.3 Low mode reweighting

As mentioned above, the conventional stochastic reweighting does not work on the larger lattice. Instead, we introduce an approximation of using only the low-lying eigenvalues. This corresponds to a certain modification of the fermion action in the ultraviolet regime. We incorporate all the eigenvalues below $\lambda \sim 100$ MeV. Here, we show that this low-mode reweighting can be used to study the gap in the Dirac spectrum.

On the smaller lattice, we compare the reweighting and the low-mode reweighting as shown in Fig. 4. Pluses and crosses represent the conventional stochastic reweighting factor and the low-mode reweighting factor, respectively. Each point represents a gauge configuration on which the reweighting factor is calculated. As the horizontal axis, we take the first eigenvalue λ_1 . Below $\lambda_1 \sim 20$ MeV, both reweighting factors are consistent and essentially zero. Configurations having near-zero modes are strongly suppressed in both reweighting techniques, and we may therefore conclude that the non-existence of the gap in the Dirac spectrum does not depend on the details of the reweighting technique.

4. Summary

We have studied the low-lying eigenvalue spectrum of the Möbius domain-wall and reweighted

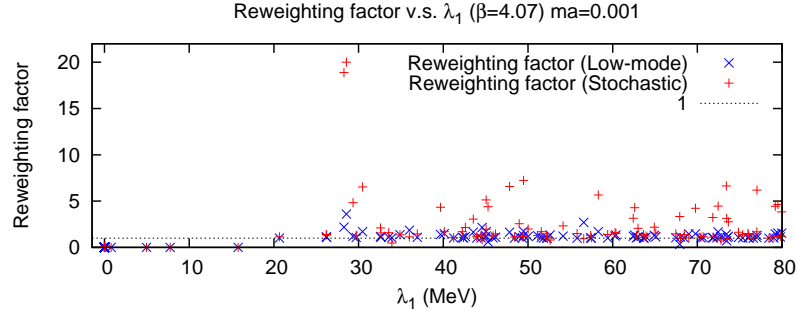


Figure 4: Reweighting factor with the low-mode reweighting (stars) and stochastic reweighting including all modes (pluses). The horizontal axis is the lowest eigenvalue of the overlap-Dirac operator for that gauge configuration. Data at $\beta = 4.07$ and $am_{ud} = 0.001$ on the $16^3 \times 8$ lattice are plotted.

overlap Dirac operators slightly above the critical temperature. Our preliminary result at the lightest quark mass shows a significant difference between them. The overlap-Dirac eigenvalue spectrum for the lightest quark mass shows a gap, which is insensitive to the volume, while that of the Möbius domain-wall has small but non-zero spectrum near $\lambda = 0$. The large violation of the Ginsparg-Wilson relation on the low-modes of the domain wall operator may explain the difference.

Numerical simulations are performed on IBM System Blue Gene Solution at KEK under a support of its Large Scale Simulation Program (No. 13/14-04). We thank H. Matsufuru for the support on the computing facility and P. Boyle for helping in the optimization of the code for BG/Q. This work is supported in part by the Grand-in-Aid of the Japanese Ministry of Education (No.25800147, No.26400259) and SPIRE (Strategic Program for Innovative Research) Field 5.

References

- [1] T. D. Cohen, Phys. Rev. D **54**, 1867 (1996).
- [2] S. Aoki, H. Fukaya and Y. Taniguchi, Phys. Rev. D **86**, 114512 (2012).
- [3] G. Cossu *et al.* [JLQCD collaboration], Phys. Rev. D **87**, no. 11, 114514 (2013).
- [4] T. W. Chiu, W. P. Chen, Y. C. Chen, H. Y. Chou and T. H. Hsieh, arXiv:1311.6220 [hep-lat].
- [5] A. Bazavov *et al.* [HotQCD Collaboration], Phys. Rev. D **86**, 094503 (2012).
- [6] M. I. Buchoff *et al.*, Phys. Rev. D **89**, 054514 (2014).
- [7] H. Ohno, U. M. Heller, F. Karsch and S. Mukherjee, PoS LATTICE **2012**, 095 (2012).
- [8] G. Cossu *et al.*, arXiv:1311.0084 [hep-lat].
- [9] R. C. Brower, H. Neff and K. Orginos, Nucl. Phys. Proc. Suppl. **140** (2005) 686;
- [10] R. C. Brower, H. Neff and K. Orginos, arXiv:1206.5214 [hep-lat]. Nucl. Phys. Proc. Suppl. **153** (2006) 191.
- [11] H. Fukaya *et al.* [JLQCD Collaboration], PoS LATTICE **2013**, 127 (2013).